



The Interdecadal Change of Relationship Between Summer Water Vapor Content Over Tibetan Plateau and Spring Sea Surface Temperature in Indian Ocean

Qian Ren^{1,2,3*}, Shanshan Zhong⁴, Dan Chen^{1,3}, Xiang Li⁵ and Tangtang Zhang²

¹Institute of Plateau Meteorology, China Meteorological Administration, Chengdu, China, ²Key Laboratory for Land Surface Process and Climate Change in Cold and Arid Regions, Chinese Academy of Sciences, Lanzhou, China, ³Heavy Rain and Drought-Flood Disasters in Plateau and Basin Key Laboratory of Sichuan Province, Chengdu, China, ⁴Key Laboratory of Meteorological Disaster, Ministry of Education, Nanjing University of Information Science and Technology, Nanjing, China, ⁵Sichuan Meteorological Observation and Data Center, Chengdu, China

OPEN ACCESS

Edited by:

Bin Yu,
Government of Canada, Canada

Reviewed by:

Zhiping Wen,
Fudan University, China
Jasti S. Chowdary,
Indian Institute of Tropical
Meteorology (IITM), India

*Correspondence:

Qian Ren
renqianxd@163.com

Specialty section:

This article was submitted to
Atmospheric Science,
a section of the journal
Frontiers in Earth Science

Received: 07 August 2020

Accepted: 12 October 2020

Published: 24 November 2020

Citation:

Ren Q, Zhong SS, Chen D, Li X and
Zhang TT, (2020) The Interdecadal
Change of Relationship Between
Summer Water Vapor Content Over
Tibetan Plateau and Spring Sea
Surface Temperature in Indian Ocean.
Front. Earth Sci. 8:592564.
doi: 10.3389/feart.2020.592564

The interannual relationship between the spring sea surface temperature over the western tropical Indian Ocean (WTIO SST) and summer water vapor content over Tibetan Plateau (TPWVC) enhances significantly after 1992/1993. The regressed atmospheric circulation against WTIO SST index (WTIO SSTI) for two periods is explored to explain the interdecadal variation. During ID1 (1979–1991), the center of the anomalous anticyclone is generally located eastward and the weak easterly anomalies on its southern flank transport moisture from the western Pacific to Southeast China with no effects on TPWVC. In ID2 (1994–2017), the Northwest Pacific anticyclone, the anomalous easterlies, and the subtropical high at 500 hPa all move westward and enhance significantly; thus, it forms a westward moisture transport pathway delivering the water vapor from the western Pacific into Tibetan Plateau. A possible mechanism is raised. On the one hand, the SST anomalies (SSTA) related to WTIO SSTI extend eastward from spring to summer in ID2. With the increased mean SST in the Indo-western Pacific Ocean under the global warming and the stronger mean summer SST in the eastern Indian Ocean, the positive SSTA induce the enhanced Kelvin waves and Northwest Pacific anticyclone with strong easterly anomalies during ID2. But in ID1, the SSTA related to WTIO SST confined in the western-central Indian Ocean from spring to summer excite the decreased Kelvin waves with less significant easterly anomalies due to the weaker mean SST. On the other hand, the eastward shift of tropical summer SSTA generates the increased convection and rising motion over the Southeast Indian Ocean in ID2. They enhance the easterly anomalies on the southern flank of the Northwest Pacific anticyclone and induce anticyclonic shear through the meridional circulation. As a result, the easterly anomalies shift westward to transport more moisture into Tibetan Plateau. However, in ID1, the easterly anomalies of the anticyclone cannot be strengthened with no westward shift. Therefore, the above reasons lead to the interdecadal enhancement of relationship between the spring WTIO SST and summer TPWVC.

Keywords: water vapor content over Tibetan Plateau, Indian Ocean sea surface temperature, enhanced interannual relationship, easterly anomalies, Northwest Pacific anticyclone, westward shift

INTRODUCTION

The Tibetan Plateau (TP) is the highest plateau in the world with the most complex terrain. Its special mechanical and thermal force especially land–atmosphere interactions determine its unique impact on climate change (Zhao and Chen, 2001a; Zhao and Chen, 2001b; Ueda et al., 2003; Zhao et al., 2018). The TP is known as “the world water tower” (Xu et al., 2008a), where there exists the maximum water vapor content above 600 hPa in summer (Wang et al., 2009; Zhou et al., 2017; Zhou et al., 2019). The TP exerts strong effects on Asian and global water cycles, thus further impacting the Asian monsoon and water vapor distribution in the downstream regions (Xu et al., 2002; Xu et al., 2008b; Chen et al., 2012; Xu et al., 2014; Curio et al., 2015). Therefore, the water vapor over the TP not only provides necessary water source for summer precipitation in the subareas and surrounding regions of the TP (Shi and Shi, 2008; Zhou et al., 2012; Zhou et al., 2015) but more importantly, it plays a robust role in summer precipitation anomalies including some extreme events in East China especially in the middle and lower reaches of the Yangtze River (Ding and Hu, 2003; Xu et al., 2003; Shi and Shi, 2008; Xu et al., 2008b; Shi et al., 2009; Zhang et al., 2013). In addition, the TP has become an important pathway for transporting water vapor from the troposphere to the stratosphere (Ye and Wu 1998; Gettelman et al., 2004; Fu et al., 2006).

A lot of studies have examined the reasons for variations of water vapor content over the TP (TPWVC). It suggests that the Asian summer monsoons as well as the subtropical westerlies are closely related with the interannual variability of the TP moisture transportation (Webster et al., 1998; Sugimoto et al., 2008; Li et al., 2009; Schiemann et al., 2009; Xie et al., 2014). However, much more vapor enters the TP through the southern boundary, and the moisture transport is much weaker at the western boundary at summertime. Thus, it presents abundant (deficient) water vapor and precipitation in the south (north) part of the TP (Liang et al., 2006; Feng and Zhou 2012; Wang et al., 2017). The moisture over the southern TP mainly comes from Arabian Sea, the Bay of Bengal, and the western Pacific Ocean (Wang et al., 2009; Chen et al., 2012; Sun and Wang 2014). An anomalous anticyclone near the south edge of the TP is the dominant factor intensifying moisture transport from the oceans to the TP (Chen et al., 2012; Feng and Zhou 2012). Besides, the North Atlantic Oscillation (NAO) can exert an effect on the interannual variation of precipitation over the TP (Liu and Chen 2000; Liu and Yin 2001; Wang et al., 2017). As far as the decadal change is concerned, it is found that the whole TP has experienced remarkable warming (Liu and Chen 2000; Wu et al., 2007; Kang et al., 2010; Moore 2012) and wetting (Xu et al., 2008a; Zhang et al., 2017; Zhou et al., 2019) at summertime in recent decades. Gao et al. (2014) state that the interdecadal growth of TP moisture is owing to the changed location of subtropical westerly jet and enhanced Asian summer monsoon

under the global warming. Zhou et al. (2019) indicate that the anomalous wave train triggered by the Atlantic SST anomalies results in the upward trend of TPWVC.

Many previous researchers have proved that the Indo-Pacific SSTA could impose profound impacts on East Asian atmospheric circulation in summer (Huang and Sun 1992; Huang et al., 2006; He and Zhu, 2015). By the means of inducing the Kelvin wave (Wu et al., 2009; Xie et al., 2009; Wu et al., 2010), positive SSTA in the equatorial Indian Ocean can give rise to a strong anomalous anticyclone over the Northwest Pacific (Chen et al., 2013; Xie et al., 2016; Tao et al., 2017; Chen et al., 2018), then affecting the water vapor transport in the lower troposphere and local precipitation (Wu et al., 2009; Wu et al., 2010; Chowdary et al., 2013; Chowdary et al., 2019). As for the TP, it is found that previous ENSO events (Li et al., 2014) and the spring SSTA in Arabian Sea (Ren et al., 2017a) could both act as precursors for the following summer moisture content in the upper troposphere of the TP. The interannual variations of TP rainfall also have a close connection with the dipole pattern of Indian Ocean SST (Bothe et al., 2010; Bothe et al., 2011). Moreover, Ji et al. (2018) reveal the relationship between spring SST in Indian Ocean and the atmospheric heat source of the TP in summer. Associated with the global warming in recent years, the interdecadal changes of Indo-Pacific SST contain not only the occurrence of ENSO modoki but also the linear warming trend of SST in the Indo-western Pacific Ocean. Both of them may lead to the interdecadal differences in the mean state of summer circulation and precipitation in East Asia (Wu and Wang, 2002; Wu et al., 2010; Wang and Mehta, 2008; Zhang et al., 2011; Kajikawa and Wang, 2012; Feng and Li, 2013; Karori et al., 2013; Zhu et al., 2014; Zhang et al., 2015). Furthermore, the interdecadal changes of relationship between the Indo-Pacific SST and precipitation in South China are also explored (Wu et al., 2012; Ren et al., 2017b).

In general, a lot of work has been done by previous studies. They focus on the interannual variation of TPWVC and its possible relationship with SST over the Indo-Pacific Ocean. They also have noticed the interdecadal change of TPWVC at mean state and put forward the possible reasons (Gao et al., 2014; Zhou et al., 2019). However, few researchers have paid more attention to the interdecadal change of relationship between TPWVC and SST. Since the spring WTIO SST are highly correlated with the summer TPWVC (Ren et al., 2017a), it is also unclear that whether their interannual relationship has undergone an interdecadal change. If it does, what factors result in this interdecadal change? Therefore, this study mainly explores the interdecadal change of the relationship between the spring WTIO SST and summer TPWVC during the different decades and its possible mechanisms.

The remaining contents of this article are organized as follows. The used datasets and principal analysis methods are introduced in *Data and Methods*. *Results* provide the all the analysis results of this paper: the *Interdecadal Change on Relationship Between*

Spring Sea Surface Temperature Over the Western Tropical Indian Ocean and Summer Water Vapor Content Over Tibetan Plateau reveals the interdecadal change of the interannual relationship between the spring WTIO SST and the summer TPWVC; *Circulation Analysis Related to the Interdecadal Change* investigates the circulation anomalies relevant to WTIO SST in the different decades; the possible physical mechanisms for the changed relation during different epochs are explored in *Possible Mechanism*. It gives a conclusion in the final section.

DATA AND METHODS

The main dataset we used for this study is the monthly mean circulation fields at 1.5° horizontal resolution provided by the European Centre for Medium-Range Weather Forecasts Interim (ERA-Interim) reanalysis (Dee et al., 2011), including geopotential height, specific humidity, zonal and meridional winds, and vertical p-velocity. Bao and Zhang (2013) have proved the advantages of ERA-Interim reanalysis data, and it has been usually used for studying the TPWVC (e.g., Gao et al., 2014; Ren et al., 2017a; Zhou et al., 2017; Zhou et al., 2019). Additional datasets consist of the monthly SST data at a $1^\circ \times 1^\circ$ global grid from Hadley Center (HadISST) (Rayner et al., 2003) and the outgoing long-wave radiation (OLR) from the National Oceanic and Atmospheric Administration (NOAA) satellite with a horizontal resolution of 2.5° (Liebmann and Smith, 1996). In this study, all the above datasets cover the period from 1979 to 2017. Summer refers to the July and August (JA), and the spring SST refers to the average SST of March, April, and May in the same year. According to the previous studies (Wang et al., 2009), July and August are the wettest month over TP, but the water vapor content in June is relatively lower. The distribution of water vapor content is consistent, and the values are roughly the same in July and August. In addition, the way in which water vapor enters TP in June is not exactly the same as that in July and August. Based on these reasons, June is not included for summer in the present work.

In this article, the water vapor content, namely, atmospheric precipitable water W (mm) over TP, refers to the calculation

method provided by the previous study (Wang et al., 2009) with the following formula:

$$W = \frac{-1}{g} \int_{P_s}^P q dp,$$

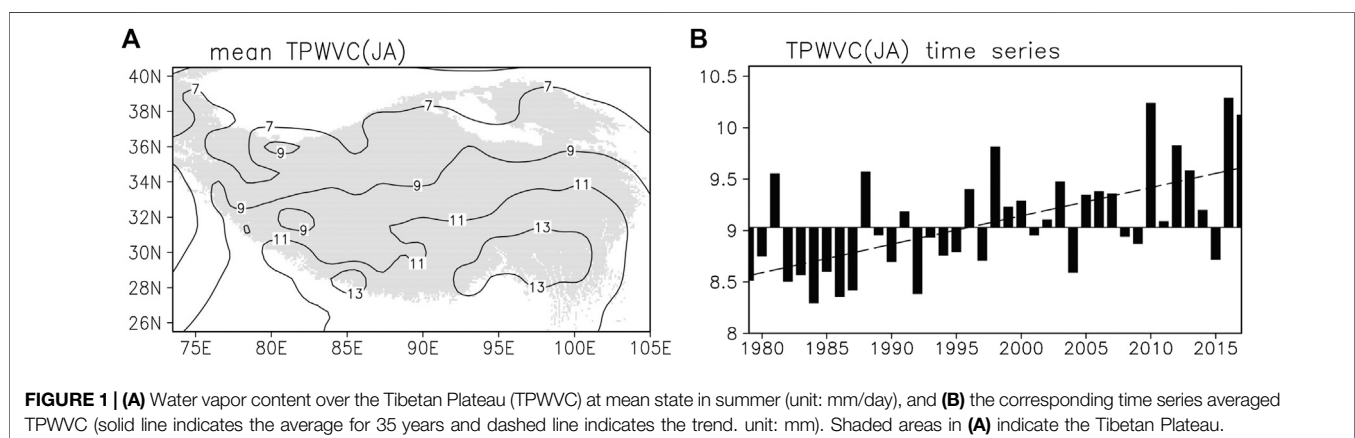
$g = 9.8 \text{ m s}^{-2}$ means the acceleration of gravity, P_s (hPa) means the surface pressure, P (hPa) identifies the top pressure, and q (kg kg^{-1}) identifies the specific humidity. As is known to all, the altitude of TP is basically beyond 600 hPa. In order to describe the features of TPWVC, if $P_s \geq 600$ hPa, it is defined as 600 hPa and P_s holds the value; if $P_s < 600$ hPa, P is defined as 100 hPa. The vertical integrated specific humidity is regarded as the estimated value of TPWVC.

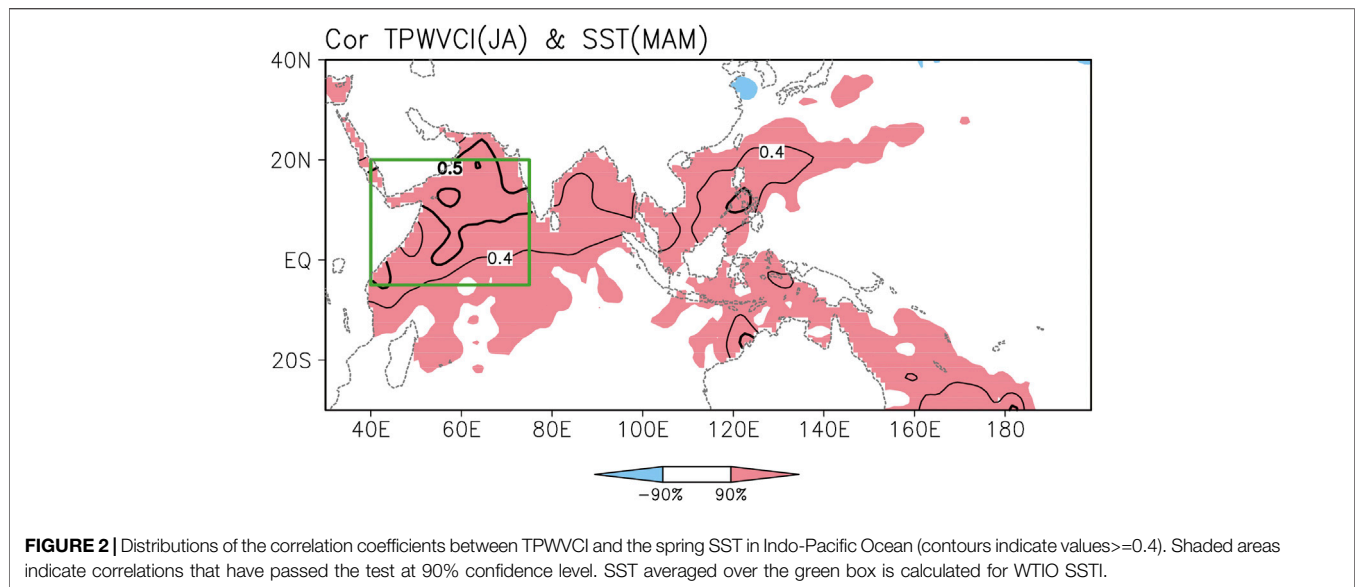
Referring to the previous definition (Ren et al., 2017a), the TP domain in the present study is defined at $25.5^\circ\text{--}40.5^\circ \text{ N}$, $73.5^\circ\text{--}105^\circ \text{ E}$. It shows that the maximum water vapor content of summer in the whole Northern Hemisphere is located in the southeast of the TP (figure not shown). Besides, there is a significant upward trend of SST over Indo-Pacific Ocean (Wang and Mehta, 2008) as well as TPWVC (Zhou et al., 2019) under the background of global warming. Before discussing the interdecadal change of relationship between WTIO SST and TPWVC, the impacts of upward trends are removed with the method of linearly detrended analysis (except **Figures 1** and **8**). Moreover, the correlation and regression analyses are applied in examining the atmospheric circulation and SSTA related to the WTIO SST and TPWVC. The Student's t test is used for assessing the statistical significance.

RESULTS

Interdecadal Change on Relationship Between Spring Sea Surface Temperature Over the Western Tropical Indian Ocean and Summer Water Vapor Content Over Tibetan Plateau

Figure 1 shows the TPWVC at mean state and the corresponding time series averaged TPWVC in summer. It presents that the





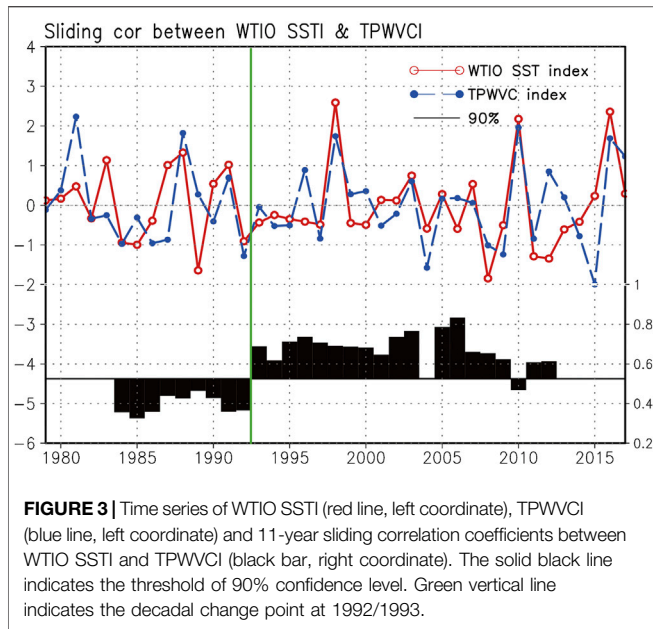
maximum TPWVC exceeds 13 mm in the southeast of TP, and it gradually decreases from southeast to northwest (**Figure 1A**). Besides, it shows the significant upward trend in the time series of TPWVC (**Figure 1B**). To eliminate the effects of linear trends, we define the linearly detrended and standardized time series in **Figure 1B** as summer TPWVC index (TPWVCI) for the following analyses.

In order to describe the relationship between the summer TPWVC and the spring WTIO SST, the temporal correlation coefficients between TPWVCI and SST over Indo-Pacific Ocean are calculated in **Figure 2**. The correlation coefficients present a consistent pattern with positive correlation in the South China Sea and the whole northern India. It indicates that warm (cold) ocean water in spring is associated with more (less) TPWVC in summer. The coefficients are much higher and present a broader shape exceeding 0.5 in the western tropical Indian Ocean. For clearly illuminating the relationship between TPWVC and WTIO SST, the standardized averaged spring SST over Indian Ocean where correlation coefficients are the highest at 5°S – 20°N , 40° – 75°E (green solid box in **Figure 2**) is defined as the WTIO SSI index (WTIO SSI).

Figure 3 presents the time series of WTIO SSI and TPWVCI in 1979–2017, and their correlation coefficient is 0.56 for the whole period exceeding the 99% confidence level. It indicates that the summer TPWVC is closely related to the spring WTIO SST. With the method mentioned before (Ren et al. 2017a), the 11-year sliding correlation coefficients (**Figure 3**) are used to investigate the interdecadal change of relationship between TPWVC and WTIO SST. It can be obviously found that there exists an interdecadal turning point of their relation at 1992/1993. It shows that the sliding correlation coefficients are quite low before 1991, which never exceed the 90% confidence level. They enhance markedly after 1993 and those of most years are significant except 2010. Here, we exclude the transition year of 1992 and 1993 in the following discussion to better distinguish the two decades. Thus, the former period from 1979 to 1991 is defined

as ID1, and the latter period from 1994 to 2017 is defined as ID2. In ID1, the correlation coefficient between WTIO SSI and TPWVCI is 0.35, not passing the test at 90% confidence level, which means weak positive interannual relation between summer TPWVC and spring WTIO SST. Comparatively, it increases remarkably to about 0.63 for ID2, exceeding the 99% confidence level. The interdecadal changes of above correlation coefficients imply that the spring WTIO SST and summer TPWVC develop a much closer interannual relationship in the latter epoch.

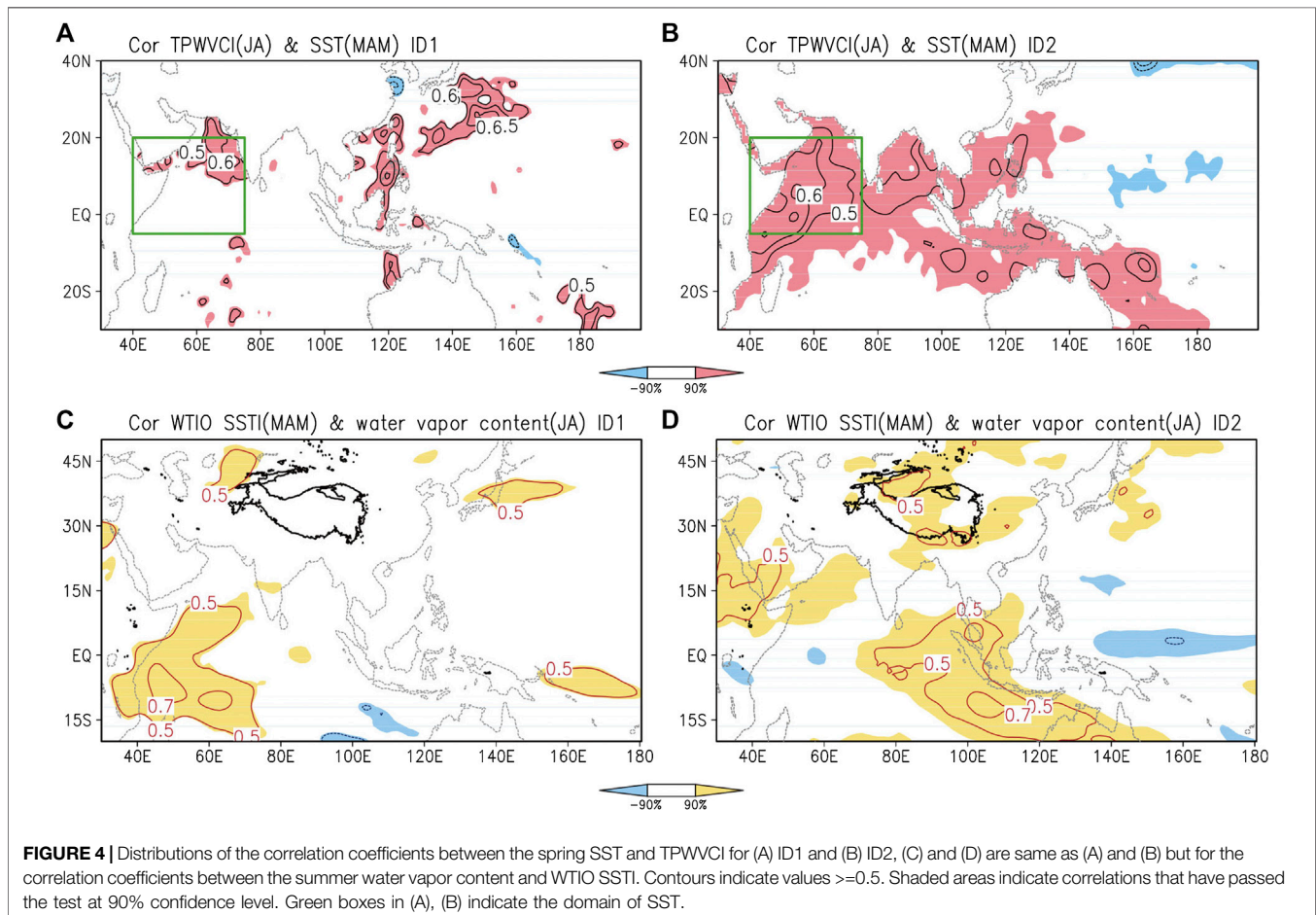
For confirming their enhanced interannual relationship, the correlation coefficients between TPWVCI and the spring SST in Indo-Pacific Ocean (**Figures 4A,B**) as well as those between WTIO SSI and the summer water vapor content (**Figures 4C,D**) at two decades are further checked. During ID1 (**Figure 4A**), it shows the weak positive SST correlation coefficients against TPWVCI in the northwest of Arabian Sea and Pacific Ocean while no significant correlation signals in other ocean areas. Comparatively, for ID2 (**Figure 4B**), it presents significantly positive correlation in almost the whole Indian Ocean, and the coefficients exceed 0.5 in large parts of regions in Arabian Sea, the Bay of Bengal, and the Southeast Indian Ocean. The high correlation between TPWVC and the SST over most of Indian Ocean indicates that TPWVC is associated with a consistent SST mode of the spring Indian Ocean Basin (IOBM). The positive correlation has a much broader shape exceeding a 90% confidence level in the WTIO SSI domain (green box in **Figure 2**), where there also exists the maximum positive correlation. Furthermore, in **Figures 4C,D**, positive correlation signals appear more significantly over the central and eastern TP during ID2, while nearly no marked correlation occurs in ID1. It also shows positive correlation coefficients over the equatorial western Indian Ocean in ID1, whereas it greatly moves eastward covering the eastern Indian Ocean in ID2. It suggests that the location of corresponding tropical convection may also experience a great interdecadal change in ID2.

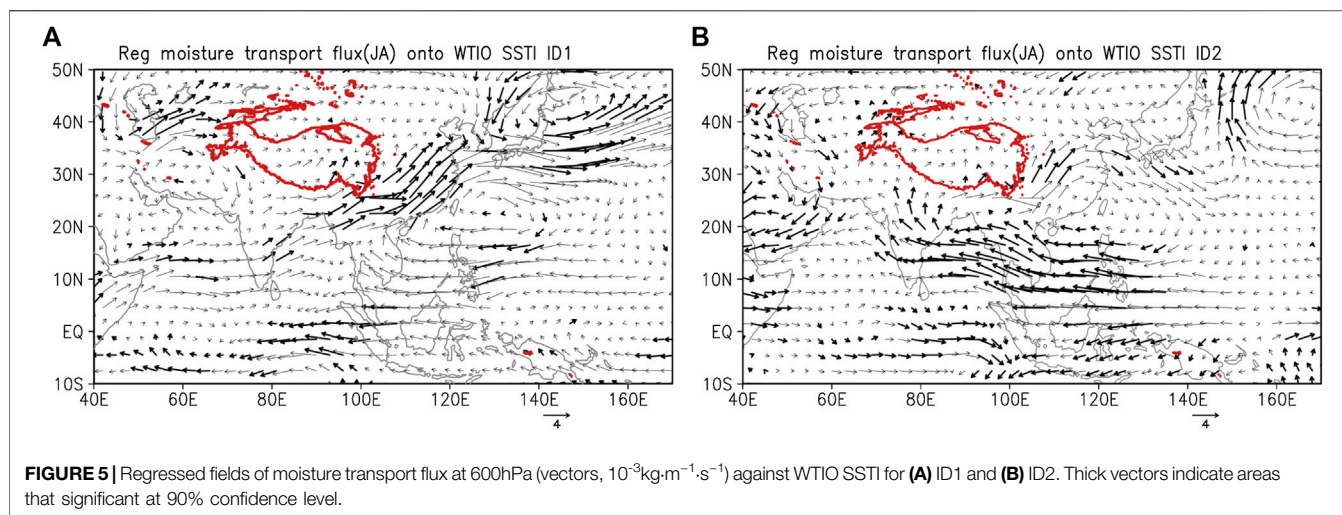


Circulation Analysis Related to the Interdecadal Change

In order to explain why the interannual relationship between TPWVCI and WTIO SST has undergone an interdecadal change, the regressed atmospheric circulation fields against WTIO SSTI for two periods are recognized in this part. In the following analysis, only the circulation variations caused by the positive WTIO SSTA are discussed. Owing to quite the opposite situations associated with the cold WTIO SSTA, it will not be repeated here.

At first, the moisture transportation which directly decides the distributions of water vapor content needs to be investigate. Thus, the regressed fields of the water vapor transport flux at 600hPa against WTIO SSTI are plotted in **Figure 5**. It shows that Northwest Pacific is occupied by the anomalous anticyclone for both ID1 (**Figure 5A**) and ID2 (**Figure 5B**) which plays an extremely important role in moisture delivery over East Asian (Wu et al., 2009; Wu et al., 2010; Chen et al., 2012; Feng and Zhou 2012). During ID1 (**Figure 5A**), the center of the anomalous anticyclone is generally located at 130° E. Influenced by the easterly anomalies on its southern flank over the Philippine Sea, water vapor is transported from the western Pacific to





Southeast China. Meanwhile, near the equator, because of the anomalous easterlies on the southern flank of anticyclonic shear centered at the Bay of Bengal, moisture originates from the Maritime Continent regions and the western Pacific, goes through the eastern Indian Ocean, turns southwesterly over the southern Indian Peninsula, and finally impacts the South China. It has no significant effect on TPWVC in the whole process of water vapor transportation. In ID2 (**Figure 5B**), it presents that the Northwest Pacific anticyclone moves westward obviously with a center at about 120°E . The anomalous easterlies over the Philippine Sea enhance notably exceeding the 90% confidence level. The anticyclonic shear located to the south of TP make great contributions to the westward extended easterly anomalies. Thus, the whole part of Indo-China Peninsula, the Bay of Bengal, and Indian Peninsula are all dominated by the strengthened easterly anomalies. They are favorable for conveying a lot of water vapor westward continuously from the western Pacific. And then, those anomalous easterlies change their direction turning southwesterly over the north Indian and transport moisture into TP through the south and west edges of TP eventually significantly leading to the increase of TPWVC.

The distributions of the regressed 850 hPa wind fields against WTIO SSTI in **Figures 6A,B** are similar with those of **Figure 5**. Compared to ID2, the anomalous Northwest Pacific anticyclone is located more eastward, and the tropical easterly anomalies would finally make an effect on the increase of water vapor content over Southeast China (not TPWVC) in ID1. During the period of ID2, the enhanced and westward moved easterly anomalies on the southern flank of anticyclone take the control of not only the Philippine Sea but also the Northeast Indian Ocean, forming a moisture transport pathway beginning from the western Pacific, going through the Indo-China Peninsula, the Bay of Bengal, and Indian Peninsula, and finally reaching the TP. Therefore, it can be concluded that the tropical easterly anomalies associated with the Northwest Pacific anticyclone exert a crucial function of increased TPWVC.

At 500 hPa geopotential height fields (**Figures 6C,D**), the subtropical high exhibits a remarkable interannual enhancement over the western Pacific whether in the former or the latter decade. However, in contrast to ID1, the positive center and its surrounding shaded areas exceeding the 90% confidence level of the regressed geopotential heights both markedly move westward covering TP during ID2. As a result, the positive anomalies over TP may conduct a great deal of ocean moisture to TP. The westward shift of regressed maximum geopotential heights is closely related to the anticyclonic shear located to the south of TP. The regressed upper winds at 150 hPa onto WTIO SSTI are calculated as well in **Figures 6E,F**. The entire TP is dominated by the westerly anomalies, and there exists an anticyclonic shear to the south of TP in the former decade. But after 1992/1993, the anomalous anticyclone presents an evidently northward movement being centered to the east of TP. It suggests that the upper divergence can be in favor of moisture convergence at the lower level over TP and then trigger the increase of TPWVC.

Possible Mechanism

Based on the above analysis of regressed circulation linked to the spring WTIO SST during two epochs, one question would be addressed that how the preceding warm SSTA makes an effect on producing the enhanced summer Northwest Pacific anticyclone and tropical easterly anomalies for two periods. The reason for the westward shift of anomalous easterlies also should be explained. Therefore, the regressed SST over Indian Ocean in spring and summer (**Figure 7**), OLR, and meridional vertical wind fields averaged $90^{\circ}\text{--}110^{\circ}\text{E}$ in summer against WTIO SSTI are plotted (**Figure 9**). Moreover, **Figure 8** shows the zonal temporal distributions of mean SST and its anomalies near the equator (averaged $15^{\circ}\text{S}\text{--}15^{\circ}\text{N}$) from 1979 to 2017.

It displays a clear distinction of the SSTA correlated with spring WTIO SST during two decades. In spring (**Figures 7A,B**), the regressed positive SSTA exceeding the 90% confidence level are located in the whole North Indian Ocean and to the west of

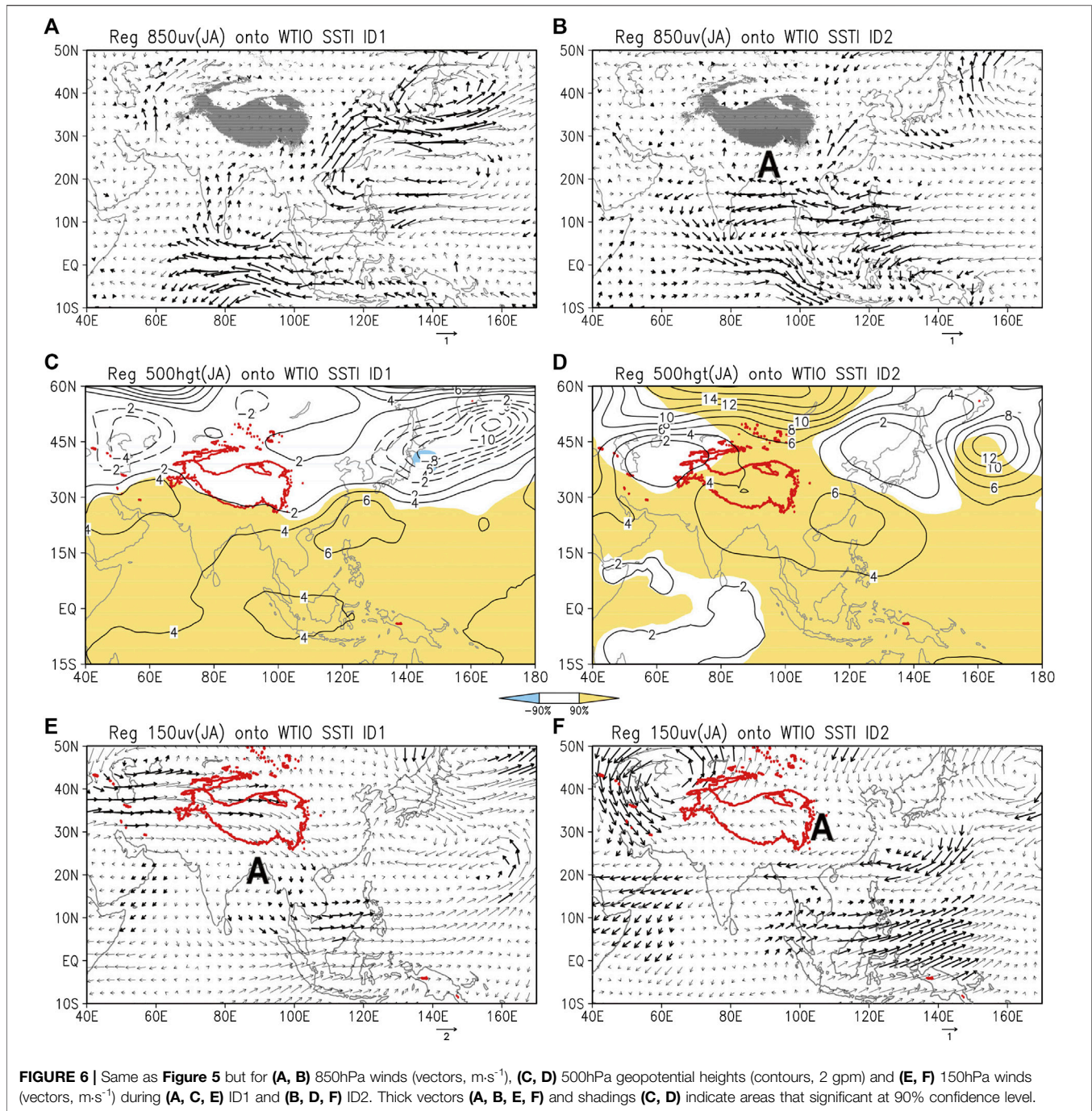
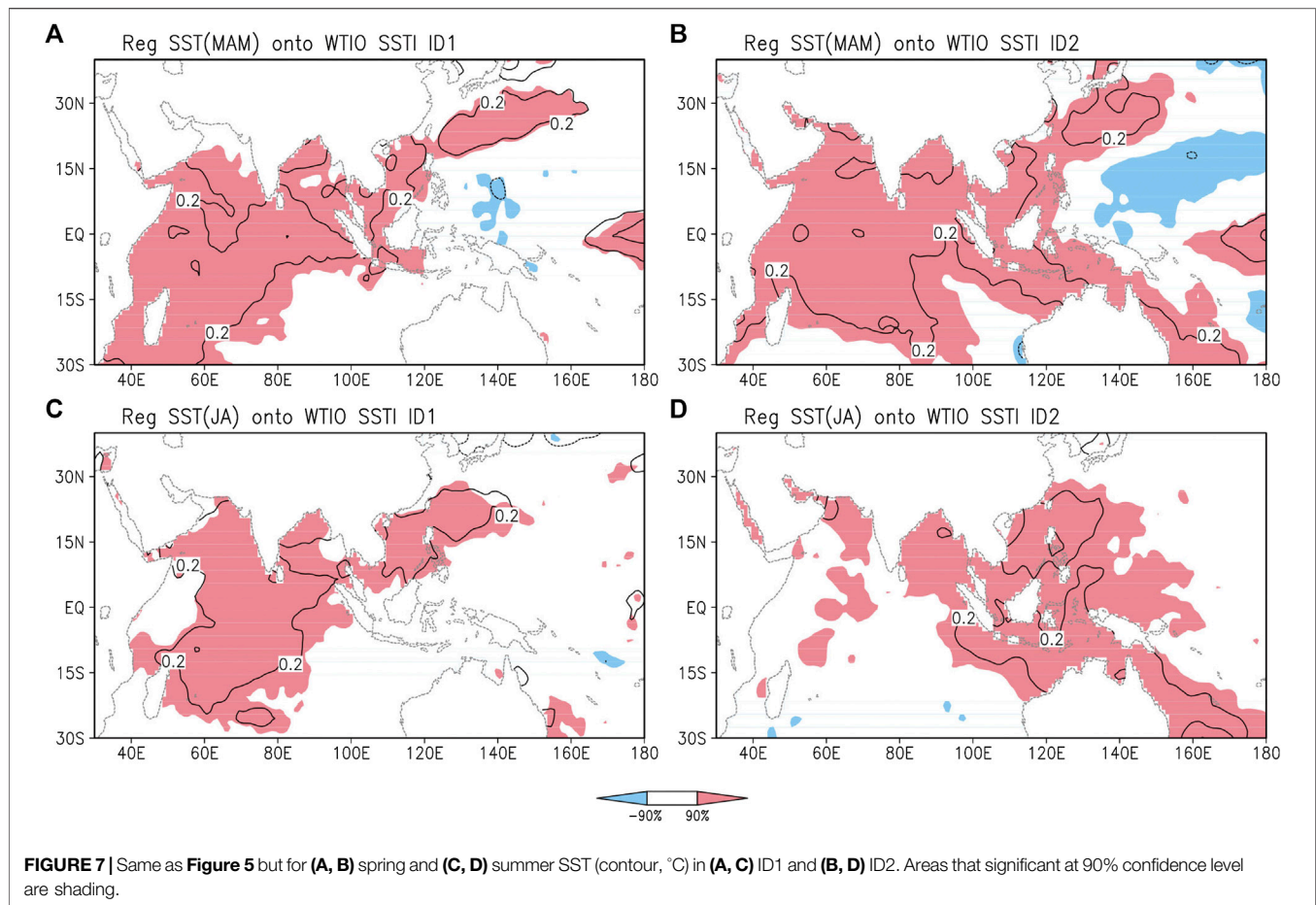


FIGURE 6 | Same as **Figure 5** but for **(A, B)** 850hPa winds (vectors, $\text{m}\cdot\text{s}^{-1}$), **(C, D)** 500hPa geopotential heights (contours, 2 gpm) and **(E, F)** 150hPa winds (vectors, $\text{m}\cdot\text{s}^{-1}$) during **(A, C, E)** ID1 and **(B, D, F)** ID2. Thick vectors **(A, B, E, F)** and shadings **(C, D)** indicate areas that significant at 90% confidence level.

80° E in the south part during the former epoch. In ID2, marked warm SSTA not only appear in the same regions of ID1 but also extend eastward, covering the Southeast Indian Ocean with an enhanced consistent mode of Indian Ocean Basin (IOBM). At summertime (**Figures 7C,D**), the significant positive anomalies of SST with a narrower scope are still confined to the western-central Indian Ocean to the west of 100° E with no obvious SSTA signals in the eastern part in ID1. Positive SSTA also occur in Northwest Pacific. However, during ID2 (**Figure 7D**), they have obviously weakened in the western

Indian Ocean, and they keep the similar distribution with that of spring in the eastern part. In addition, SST is also positively linked to WTIO SSTI in the Northwest Pacific and the Maritime Continent. The regressed significant SSTA in summer move eastward and may provide a more important impact on circulation. Besides, for both epochs, the warm SSTA in Indian Ocean can trigger the Kelvin waves in summer. Those waves impose a profound impact on generating the anomalous Northwest Pacific anticyclone and do a great favor for moisture transportation. The enhanced SSTA in the Maritime Continent

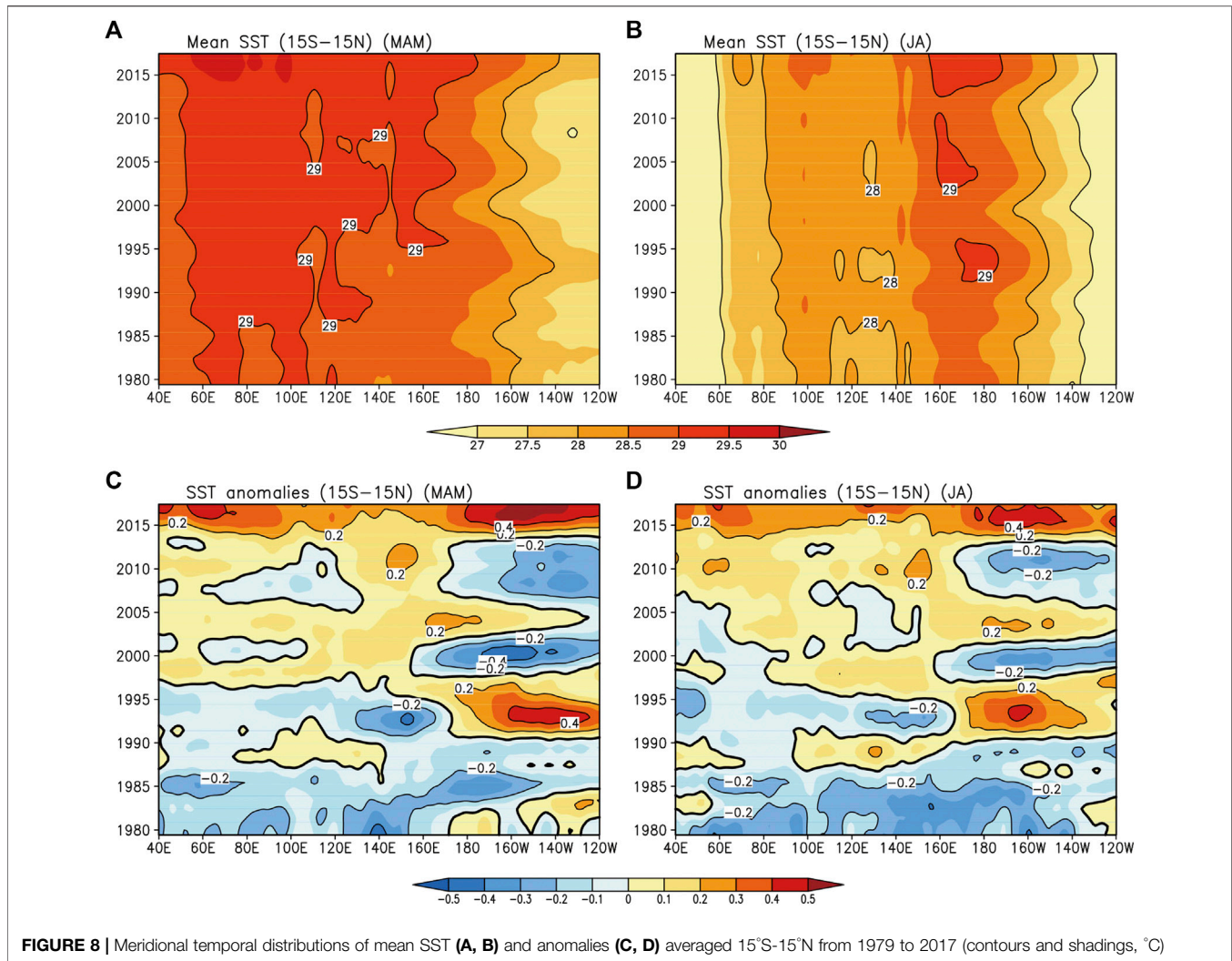


indicate the stronger Kelvin waves and the anomalous anticyclone during ID2.

In **Figures 8A,B**, SST is much warmer in summer over the equatorial Indo-Pacific Ocean. The regions of SST higher than 29°C in spring for ID1 only dominate the west-central Indian Ocean. They expand eastward covering the areas of 110°–180° E for ID2. The SST increases significantly over the Indo-Pacific Ocean, especially the eastern Indian and western Pacific Ocean (**Figure 8C**). It explains why the correlation signals of spring SST against TPWVCI (**Figure 4B**) are much stronger than those in summer (figure not shown). Compared to that in spring, the SST center of Indian Ocean is anchored in the east at summertime during the entire period (**Figure 8B**) with the seasonal decrease of maximum SST. The SST in the eastern Indian Ocean exceeds 28°C, but not in the western part. It also shows an interdecadal enhancement of SST (**Figure 8D**) and its broader scopes (higher than 28°C) (**Figure 8B**) over the eastern Indian Ocean and western Pacific Ocean during ID2.

Based on **Figures 8C,D**, it is clear that the mean SST has already enhanced from spring to summer in the Indo-Pacific Ocean for the latter epoch. Previous study has proved that IOBM has become much stronger under the background of global warming (Zheng et al., 2011; Tao et al., 2015; Hu et al., 2014). It may be associated with El Niño. The correlation coefficient between WTIO SSTI and the Niño 3.4 index of preceding winter is 0.83 and 0.81 for ID1 and

ID2, respectively. Tao et al. (2015) and Hu et al. (2014) indicate that the effects of SSTA on the water vapor are nonlinear. With warmer mean SST, the same intensity of El Niño can induce the much stronger anomalous water vapor for ID2. Then, they give rise to the enhanced eastward propagating Kelvin waves and warmer tropospheric temperature, further resulting in the stronger IOBM in ID2. So the SSTA associated with WTIO SSTI already extend eastward, covering the Southeast Indian Ocean in the spring of ID2. When it turns to summer, mean SST becomes much warmer in ID2 (**Figure 8D**), the IOBM is still much stronger than that in ID1. As the mean summer SST in the eastern Indian Ocean is stronger than that in the western part (**Figure 8B**), the positive SSTA in the eastern Indian Ocean excite the enhanced Kelvin waves and Northwest Pacific anticyclone with increased easterly anomalies during ID2. In turn, they also help maintain the SSTA of the eastern Indian Ocean by the easterly anomalies. In addition, the intensity of mean SST has obviously decreased in contrast with that in spring (**Figures 8B**), resulting in the weakened IOBM. Therefore, the warmer SSTA can be easier to continuously exist in the eastern Indian Ocean and gradually decrease in the west. However, the SST at mean state of ID1 are still relatively weaker in summer and located to the west. The SSTA in **Figure 7C** trigger the decreased Kelvin waves with less significant easterly anomalies. The SSTA related to WTIO SSTI keep staying in the western-central Indian Ocean with a slightly narrower scope.

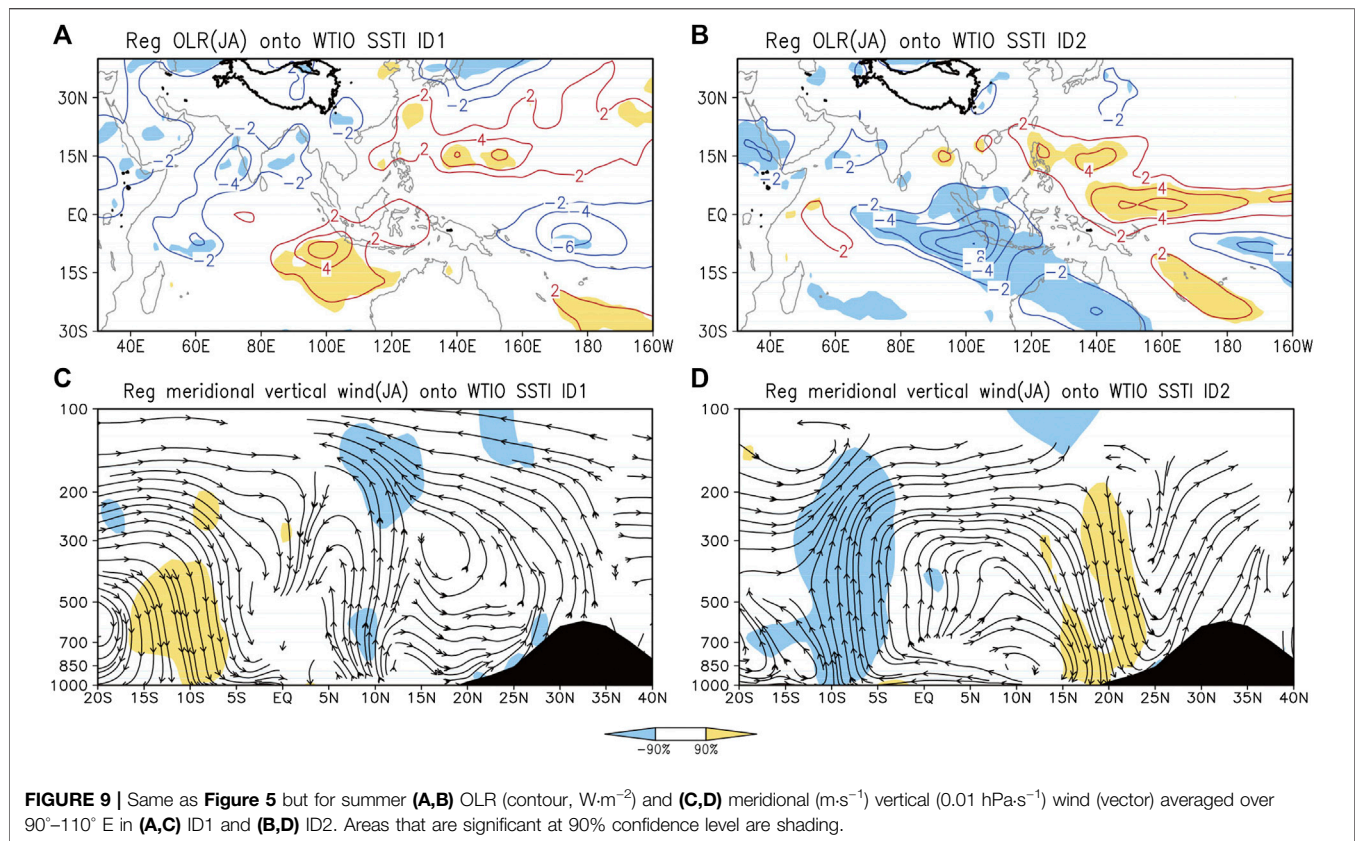


Therefore, the SSTA during summer connect with the spring WTIO SST are totally different for the two periods.

The distributions of regressed OLR onto WTIO SSTI are plotted to illuminate the corresponding characteristics of convection anomalies (**Figures 9A,B**). During the former period (**Figure 9A**), it exhibits a triple pattern (negative-positive-negative from west to east) over the tropical Indo-Pacific Ocean. Corresponding to the significant positive SSTA, the enhanced convection with anomalous ascending motion is induced in the western Indian Ocean, and then the anomalous zonal vertical circulation is driven. As a result, it produces the decreased convection with sinking branch over the Southeast Indian Ocean centered around 100° E and makes low-level easterly anomalies mainly confined to the equatorial Indian Ocean (**Figure 6A**). Due to the further south position of these easterly anomalies, more water vapor cannot be conveyed into TP. The convective subsidence is strengthened in Northwest Pacific because of the anticyclone triggered by Kelvin waves, but it only reaches 120° E to the west (**Figure 9A**). Besides, vertical wind fields averaged 90°–110° E in summer against WTIO SSTI are checked to study the local

meridional circulation (**Figures 9C,D**). As the downdrafts occur over the Southeast Indian Ocean, upward movement is stimulated from 5° N to TP (**Figure 9C**). It indicates that the Northwest Pacific anticyclone is located eastward.

By comparison, during the period of ID2 (**Figure 9B**), the anomalous convection presents a tropical opposite pattern in Indo-Pacific Ocean with notably enhanced rising motion over the Southeast Indian Ocean and the Maritime Continent, and marked sinking branch over the central Pacific. On the one hand, the ascending branch response to the intense positive SSTA in the Southeast Indian Ocean and the Maritime Continent (**Figure 7D**) drives the strengthened anomalous zonal vertical circulation. It gives rise to the tropical subsidence in the central Pacific around 160° E. Thus, the anomalous easterlies that are responsible for the moisture transport are significantly induced from the eastern Indian Ocean to the western Pacific (**Figure 6B**), strengthening the easterly anomalies on the southern flank of the Northwest Pacific anticyclone. On the other hand, the updrafts over the Southeast Indian Ocean and the Maritime Continent also trigger



the local meridional circulation, which results in the downdrafts just located to the south of TP from 15° to 25° N (**Figure 9D**). The induced anticyclonic shear by the downdrafts over there can lead to the westward shift of easterly anomalies on the southern flank of the Northwest Pacific anticyclone reaching the Bay of Bengal and the Indian Peninsula, and then turning southerly anomalies to transport the moisture to TP.

Therefore, we can put forward a possible mechanism for the enhanced relationship between WTIO SST and TPWVC drawing conclusions from the above analysis. On the one hand, under the background of global warming, the mean SST increases from spring to summer in the Indo-western Pacific Ocean, and the IOBM has become much stronger. The SSTA associated with WTIO SSTI extend eastward covering the Southeast Indian Ocean from spring to summer in ID2. With the stronger mean summer SST in the eastern Indian Ocean, the positive SSTA there induce the enhanced Kelvin waves and Northwest Pacific anticyclone with increased easterly anomalies during ID2. In turn, they help maintain the SSTA of the eastern Indian Ocean by the easterly anomalies. However, owing to the weaker mean SST, the SSTA related to WTIO SST keep staying in the western-central Indian Ocean from spring to summer trigger the decreased Kelvin waves with less significant easterly anomalies during ID1.

On the other hand, it suggests that positive SSTA are more likely to induce the much stronger convection with anomalous ascending motion over the eastern part of Indian Ocean in summer for ID2. It drives the strengthened anomalous zonal

vertical circulation and induces the anomalous easterlies on the southern flank of the Northwest Pacific anticyclone which are responsible for the moisture transport. Furthermore, it results in the downdrafts and triggers anticyclonic shear to the south of TP through the meridional circulation. Finally, the increased easterly anomalies of the Northwest Pacific anticyclone shift westward across the Bay of Bengal to transport the moisture to TP. But in ID1, downdrafts occur over the Southeast Indian Ocean with upward movement in the western Indian Ocean. The triggered zonal vertical circulation cannot strengthen the easterly anomalies in the south of the weaker Northwest Pacific anticyclone. The induced rising motion to the south of TP cannot help the Northwest Pacific anticyclone move westward. Finally, it leads to easterly anomalies confined in the equatorial Indian Ocean with no effects on TPWVC in ID1. Results from the above reasons, the easterly anomalies responsible for transporting moisture to TPWVC shift westward and finally lead to the enhanced interannual relationship between the spring WTIO SST and summer TPWVC after 1992/1993.

CONCLUSIONS

The interdecadal variation of interannual relationship between the spring WTIO SST and summer TPWVC is mainly studied in this article. The sliding correlation coefficients show that their relation enhances significantly after 1992/1993. Thus, the former period from 1979 to 1991 is defined as ID1, and the latter from

1994 to 2017 is defined as ID2. In ID1, the correlation coefficient between the spring WTIO SSTI and summer TPWVCI is 0.35 not passing the test at 90% confidence level, indicating their weak positive interannual relation. Comparatively, it increases obviously to about 0.63 for ID2 exceeding the 99% confidence level.

The regressed atmospheric circulation fields against WTIO SSTI for two periods are investigated. During ID1, the center of the anomalous anticyclone at 850 hPa is generally located eastward at 130° E. Influenced by the easterly anomalies on its southern flank, water vapor is transported from the western Pacific Ocean to Southeast China, but it has no significant effect on TPWVC. In ID2, the Northwest Pacific anticyclone moves westward significantly. The anomalous easterlies on its southern flank enhance notably and shift westward with the effects of the anticyclonic shear to the south of TP. Thus, the easterly anomalies transport a lot of water vapor westward continuously from the western Pacific; go through the Indo-China Peninsula, the Bay of Bengal, and Indian Peninsula; and eventually reach TP significantly leading to the increased TPWVC. Besides, the enhanced subtropical high at 500 hPa in summer over the western Pacific also markedly move westward during ID2, conducting a great deal of ocean moisture to TP. At 150 hPa wind field, the anomalous anticyclone to the south of TP in ID1 move northward to be centered at Southeast TP in ID2. The upper divergence of TP can do a favor for moisture convergence at the lower level and finally trigger the enhancement of TPWVC. Given that the easterly anomalies of the Northwest Pacific anticyclone are of great significance to moisture transportation, their westward movement and increased intensity during ID2 eventually lead to the enhancement of TPWVC.

A possible mechanism is raised for explaining the enhancement and westward shift of easterly anomalies related to the spring WTIO SST in ID2. On one side, the mean SST increases from spring to summer in the Indo-western Pacific Ocean under the global warming. The SSTA linked with WTIO SSTI extend eastward, covering the Southeast Indian Ocean from spring to summer in ID2. With the stronger mean summer SST in the eastern Indian Ocean, the positive SSTA induce the enhanced Kelvin waves and Northwest Pacific anticyclone with increased easterly anomalies during ID2. But in ID1, the SSTA related to WTIO SST confined in the western-central Indian Ocean from spring to summer excite the decreased Kelvin waves with less significant easterly anomalies due to the weaker mean SST. On the other side, because the positive summer SSTA are located in the eastern/western Indian Ocean, the increased/decreased

convection and rising/sinking motion are induced over the Southeast Indian Ocean in ID2/ID1. It gives rise to the downdrafts/updrafts in Central Pacific to enhance/weaken the easterly anomalies on the southern flank of the Northwest Pacific anticyclone. Furthermore, it can result in the downdrafts/updrafts to the south of the TP by inducing the local meridional circulation for ID2/ID1. It further generates the anticyclonic shear over there resulting in the westward shift of the easterly anomalies to transport more moisture into TP in ID2 compared with no obvious westward shifted easterly anomalies of anticyclone and no vapor transportation to TP in ID1. As a result of the above reasons, the interannual relationship between the spring WTIO SST and summer TPWVC has significantly enhanced after 1992/1993.

DATA AVAILABILITY STATEMENT

Publicly available datasets were analyzed in this study. This data can be found here: <https://apps.ecmwf.int/datasets/data/interim-full-moda/levtype=sfc/>.

AUTHOR CONTRIBUTIONS

QR performed tropical air-sea interaction, and data and figures processing; SSZ performed correlation between heating of the Tibetan Plateau and tropical thermal forcing; DC performed the analysis of water vapor content over Tibetan Plateau; XL performed data processing and TTZ performed climate variability in the Tibetan Plateau.

FUNDING

This work was supported by the Innovation Team Project (grant number BROP202043) of Institute of Plateau Meteorology, CMA: Opening Fund of Key Laboratory for Land Surface Process and Climate Change in Cold and Arid Regions, CAS (LPCC2018004); the cosponsored project by Sichuan Meteorological Bureau and Nanjing University of Information Science & Technology (SCJXHZ04); the Strategic Priority Research Program of Chinese Academy of Sciences (XDA20100300); the Second Tibetan Plateau Scientific Expedition and Research program (Grant 2019QZKK0106); the National Natural Science Foundation of China (41775084).

REFERENCES

- Bao, X. H., and Zhang, F. H. (2013). Evaluation of NCEP-CFSR, NCEP-NCAR, ERA-interim, and ERA-40 reanalysis datasets against independent sounding observations over the Tibetan plateau. *J. Clim.* 26, 206–214. doi:10.1175/JCLI-D-12-00056.1
- Bothe, O., Fraedrich, K., and Zhu, X. H. (2010). The large-scale circulations and summer drought and wetness on the Tibetan plateau. *Int. J. Climatol.* 30, 844–855. doi:10.1002/joc.1946
- Bothe, O., Fraedrich, K., and Zhu, X. H. (2011). Large-scale circulations and Tibetan Plateau summer drought and wetness in a high-resolution climate model. *Int. J. Climatol.* 31, 832–846. doi:10.1002/joc.2124
- Chen, B., Xu, X. D., Yang, S., and Zhang, W. (2012). On the origin and destination of atmospheric moisture and air mass over the Tibetan Plateau. *Theor. Appl. Climatol.* 110, 423–435. doi:10.1007/s00704-012-0641-y
- Chen, J. P., Wang, X., Zhou, W., and Wen, Z. P. (2018). Interdecadal change in the summer SST-precipitation relationship around the late 1990s over the South China Sea. *Clim. Dynam.* 51, 2229–2246. doi:10.1007/s00382-017-4009-y

- Chen, W., Feng, J., and Wu, R. G. (2013). Roles of ENSO and PDO in the link of the East Asian winter monsoon to the following summer monsoon. *J. Clim.* 26, 622–635. doi:10.1175/JCLI-D-12-00021.1
- Chowdary, J. S., Gnanaseelan, C., and Chakravorty, S. (2013). Impact of northwest Pacific anticyclone on the Indian summer monsoon region. *Theor. Appl. Climatol.* 113, 329–336. doi:10.1007/s00704-012-0785-9
- Chowdary, J. S., Patekar, D. D., Srinivas, G., Gnanaseelan, C., and Parekh, A. (2019). Impact of the indo-western Pacific Ocean capacitor mode on south asian summer monsoon rainfall. *Clim. Dynam.* 53, 2327–2338. doi:10.1007/s00382-019-04850-w
- Curio, J., Maussion, F., and Scherer, D. (2015). A 12-year high-resolution climatology of atmospheric water transport over the Tibetan Plateau. *Earth Syst Dynam.* 6, 109–124. doi:10.5194/esd -6-109-2015
- Dee, D. P., Uppala, S. M., Simmons, A. J., Berrisford, P., Poli, P., Kobayashi, S., et al. (2011). The ERA-Interim reanalysis: configuration and performance of the data assimilation system. *Quart J Roy Meteor Soc.* 137, 553–597. doi:10.1002/qj.828
- Ding, Y. H., and Hu, G. Q. (2003). A study on water vapor budget over China during the 1998 severe flood periods (in Chinese). *Acta Meteorol. Sin.* 61(2), 129–145. doi:10.11676/qxxb2003.014
- Feng, J., and Li, J. P. (2013). Influence of El niño modoki on spring rainfall over South China. *J. Geophys. Res. Atmos.* 116, D13102. doi:10.1029/2010JD015160
- Feng, L., and Zhou, T. J. (2012). Water vapor transport for summer precipitation over the Tibetan Plateau: multi-dataset analysis. *J. Geophys. Res. Atmos.* 117, D20114. doi:10.1029/2011JD017012
- Fu, R., Hu, Y. L., Wright, J. S., Jiang, J. H., Dickinson, R. E., Chen, M. X., et al. (2006). Short circuit of water vapor and polluted air to the global stratosphere by convective transport over the Tibetan Plateau. *Proc. Natl. Acad. Sci. U.S.A.* 103, 5664–5669. doi:10.1073/pnas.06015 841-03
- Gao, Y. H., Lan, C., and Zhang, Y. X. (2014). Changes in moisture flux over the Tibetan Plateau during 1979–2011 and possible mechanisms. *J. Clim.* 27, 1876–1893. doi:10.1175/JCLI-D-13- 00321.1
- Gottelman, A., Kinnison, D. E., Dunkerton, T. J., and Brasseur, G. P. (2004). Impact of monsoon circulations on the upper troposphere and lower stratosphere. *J. Geophys. Res. Atmos.* 109, 51–67. doi:10.1029/2004JD004878
- He, J. H., and Zhu, Z. W. (2015). The relation of South China Sea monsoon onset with the subsequent rainfall over the subtropical East Asia. *Int. J. Climatol.* 35, 4547–4556. doi:10.1002/joc.4305
- Hu, K. M., Huang, G., Zheng, X. T., and Xie, S. P. (2014). Interdecadal variations in ENSO influences on northwest Pacific–East Asian early summertime climate simulated in CMIP5 models. *J. Clim.* 27, 5982–5998. doi:10.1175/JCLI-D-13-00268.1
- Huang, R. H., Gu, L., Zhou, L. T., and Wu, S. S. (2006). Impact of the thermal state of the tropical western Pacific on onset date and process of the South China Sea summer monsoon. *Adv. Atmos. Sci.* 23(6), 909–924. doi:10.1007/s00376-006-0909-1
- Huang, R. H., and Sun, F. Y. (1992). Impacts of the tropical western Pacific on the East Asian summer monsoon. *J. Meteorol. Soc. Jpn.* 70, 243–256. doi:10.2151/jmsj1965.70.1b_243
- Ji, C. X., Zhang, Y. Z., Cheng, Q. M., Li, Y., Jiang, T. C., and Liang, X. S. (2018). On the relationship between the early spring Indian Ocean's sea surface temperature (SST) and the Tibetan Plateau atmospheric heat source in summer. *Global Planet. Change.* 164, 1–10. doi:10.1016/j.gloplacha.2018.02.011
- Kajikawa, Y., and Wang, B. (2012). Interdecadal change of the South China Sea summer monsoon onset. *J. Clim.* 25, 3207–3218. doi:10.1175/jcli-d-11-00207.1
- Kang, S. C., Xu, Y. W., You, Q. L., Flügel, W. A., Pepin, N., and Yao, T. D. (2010). Review of climate and cryospheric change in the Tibetan Plateau. *Environ. Res. Lett.* 5, 015101. doi:10.1088/1748- 9326/5/1/015101
- Karori, M. A., Li, J. P., and Jin, F. F. (2013). The asymmetric influence of the two types of El Niño and La Niña on summer rainfall over southeast China. *J. Clim.* 26, 4567–4582. doi:10.1175/JCLI-D-12-00324.1
- Li, M. J., Zhang, X. Q., and Xie, C. Y. (2014). Cause analysis on typical abnormal year of water vapor in the upper troposphere over Qinghai-Xizang Plateau (in Chinese). *Plateau Meteorol.* 8(1), 1197–1203. doi:10.7522/j.issn.1000-0534. 2013.00111
- Li, S. C., Li, D. L., Zhao, P., and Zhang, G. Q. (2009). The climatic characteristics of vapor transportation in rainy season of the origin area of three rivers in Qinghai-Xizang Plateau (in Chinese). *Acta Meteorol. Sin.* 67(4), 591–598. doi:10.11676/qxxb2009.059
- Liang, H., Liu, J. M., and Li, S. K. (2006). Analysis of precipitable water vapor source distribution and its seasonal variation characteristics over Tibetan Plateau and its surroundings (in Chinese). *J. Nat. Resour.* 21(4), 526–534. doi:10.33 21/j.issn: 1000-3037.2006.04.004
- Liebmann, B., and Smith, C. A. (1996). Description of a complete (interpolated) outgoing longwave radiation dataset. *Bull. Am. Meteorol. Soc.* 77, 1275–1277. doi:10.1175/15200477(1996)077<1255:EA>2.0. CO;2
- Liu, X. D., and Chen, B. D. (2000). Climatic warming in the Tibetan Plateau during recent decades. *Int. J. Climatol.* 20, 1729–1742. doi:10.1002/1097-0088(20001130) 20:14<1729::AID-JOC556> 3.0.CO;2-Y
- Liu, X. D., and Yin, Z. Y. (2001). Spatial and temporal variation of summer precipitation over the eastern Tibetan plateau and the North Atlantic Oscillation. *J. Clim.* 14, 2896–2909. doi:10.1175/1520-0442(2001)014<2896: SATVOS>2.0.CO;2
- Moore, G. W. K. (2012). Surface pressure record of Tibetan Plateau warming since the 1870s. *Quart J Roy Meteor Soc.* 138, 1999–2008. doi:10.1002/qj. 1948
- Rayner, N. A., Parker, D. E., Horton, E. B., Folland, C. K., Alexander, L. V., Rowell, D. P., et al. (2003). Global analyses of sea surface temperature, sea ice, and night marine air temperature since the late nineteenth century. *J. Geophys. Res. Atmos.* 108. doi:10.1029/2002jd002670
- Ren, Q., Zhou, C. Y., He, J. H., Cen, S. X., and Deng, M. Y. (2017a). Impact of preceding Indian Ocean sea surface temperature anomaly on water vapor content over the Tibetan Plateau moist pool in summer and its possible reason (in Chinese). *Chin. J. Atmos. Sci.* 41(3), 648–658. doi:10.3878/j.issn.1006-9895. 1610.16161
- Ren, Q., Zhu, Z. W., Hao, L. P., and He, J. H. (2017b). The enhanced relationship between Southern China winter rainfall and warm pool ocean heat content. *Int. J. Climatol.* 37, 409–419. doi:10.1002/joc.4714
- Schiemann, R., Lüthi, D., and Schär, C. (2009). Seasonality and interannual variability of the westerly jet in the Tibetan Plateau region. *J. Clim.* 22, 2940–2957. doi:10.1175/2008JCLI2625.1
- Shi, X. Y., and Shi, X. H. (2008). Climatological characteristics of summertime moisture budget over the southeast part of Tibetan Plateau with their impacts (in Chinese). *J. Appl. Meteorol. Sci.* 19(1), 41–46. doi:10.3969/j.issn.1001-7313. 2008.01.006
- Shi, X. H., Xu, X. D., and Cheng, X. H. (2009). Premonitory of water vapor transport in the upstream key region over the Tibetan Plateau during the 2008 snowstorm disaster in South China (in Chinese). *Acta Meteorol. Sin.* 67 (3), 478–487. doi:10.3321/j. issn:0577-6619.2009.03.015
- Sugimoto, S., Ueno, K., and Sha, W. (2008). Transportation of water vapor into the Tibetan Plateau in the case of a passing synoptic-scale trough. *J. Meteorol. Soc. Jpn.* 86, 935–949. doi:10.2151/jmsj.86.935
- Sun, B., and Wang, H. J. (2014). Moisture sources of semiarid grassland in China using the Lagrangian particle model FLEXPART. *J. Clim.* 27, 2457–2474. doi:10. 1175/JCLI-D-13-00517.1
- Tao, L., Li, T., Ke, Y. H., and Zhao, J. W. (2017). Causes of interannual and interdecadal variations of the summertime Pacific-Japan-like pattern over East Asia. *J. Climate.* 30, 8845–8864. doi:10.1175/JCLI-D-15-0817.1
- Tao, W. C., Huang, G., Hu, K. M., Qu, X., Wen, G. H., and Gong, H. N. (2015). Interdecadal modulation of ENSO teleconnections to the Indian Ocean Basin Mode and their relationship under global warming in CMIP5 models. *Int. J. Climatol.* 35(3), 391–407. doi:10.1002/joc.3987
- Ueda, H., Kamahori, H., and Yamasaki, N. (2003). Seasonal contrasting features of heat and moisture budgets between the eastern and western Tibetan Plateau during the GAME IOP. *J. Clim.* 16, 2309–2324. doi:10.1175/ 2757.1
- Wang, H., and Mehta, V. (2008). Decadal variability of the Indo-Pacific warm pool and its association with atmospheric and oceanic variability in the NCEP-NCAR and SODA reanalyses. *J. Clim.* 21, 5545–5565. doi:10.1175/ 2008JCLI2049.1
- Wang, X., Gong, Y. F., and Cen, S. X. (2009). Characteristics of the moist pool and its moisture transports over Qinghai-Xizang Plateau in summer half year (in Chinese). *Acta Geograph. Sin.* 64(5), 601–608. doi:10.11821/xb200905009
- Wang, Z. Q., Duan, A. M., Yang, S., and Ullah, K. (2017). Atmospheric moisture budget and its regulation on the variability of summer precipitation over the Tibetan Plateau. *J. Geophys. Res. Atmos.* 122, 614–630. doi:10.1002/ 2016JD025515

- Webster, P. J., Magana, V. O., Palmer, T. N., Shukla, J., Tomas, R. A., Yanai, M., et al. (1998). Monsoons: processes, predictability, and the prospects for prediction. *J. Geophys. Res. Atmos.* 103, 14451–14510. doi:10.1029/97JC02719
- Wu, B., Li, T., and Zhou, T. J. (2010). Relative contributions of the Indian Ocean and local SST anomalies to the maintenance of the western North Pacific anomalous anticyclone during the El Niño decaying summer. *J. Clim.* 23, 2974–2986. doi:10.1175/2010JCLI3300.1
- Wu, B., Zhou, T. J., and Li, T. (2009). Seasonally evolving dominant interannual variability modes of East Asian climate. *J. Clim.* 22, 2992–3005. doi:10.1175/2008JCLI2710.1
- Wu, R. G., and Wang, B. (2002). A contrast of the east asian summer monsoon-ENSO relationship between 1962-77 and 1978-93. *J. Clim.* 22, 3266–3279. doi:10.1175/1520-0442(2002)015<3266:ACOTEA>2.0.CO;2
- Wu, R. G., Wen, Z. P., Yang, S., and Li, Y. H. (2010). An interdecadal change in southern China summer rainfall around 1992-93. *J. Clim.* 23, 2389–2403. doi:10.1175/2009JCLI3336.1
- Wu, R. G., Yang, S., Wen, Z. P., Huang, G., and Hu, K. M. (2012). Interdecadal change in the relationship of southern China summer rainfall with tropical Indo-Pacific SST. *Theor. Appl. Climatol.* 108, 119–133. doi:10.1007/s00704-011-0519-4
- Wu, S. H., Yin, Y. H., Zheng, D., and Yang, Q. Y. (2007). Climatic trends over the Tibetan plateau during 1971-2000. *J. Geogr. Sci.* 17, 141–151. doi:10.1007/s11442-007-0141-7
- Xie, C. Y., Li, M. J., and Zhang, X. Q. (2014). Characteristics of summer atmospheric water resources and its causes over the Tibetan Plateau in recent 30 Years (in Chinese). *J. Nat. Resour.* 29 (6), 979–989. doi:10.11849/zrzyxb.2014.06.007
- Xie, S. P., Hu, K. M., Hafner, J., Tokinaga, H., Du, Y., Huang, G., et al. (2009). Indian ocean capacitor effect on indo-western pacific climate during the summer following El Niño. *J. Clim.* 22: 730–747. doi:10.1175/2008JCLI2544.1
- Xie, S. P., Kosaka, Y., Du, Y., Hu, K. M., Chowdary, J. S., and Huang, G. (2016). Indo-western Pacific Ocean capacitor and coherent climate anomalies in post-ENSO summer: a review. *Adv. Atmos. Sci.* 33, 411–432. doi:10.1007/s00376-015-5192-6
- Xu, X. D., Lu, C. G., Shi, X. H., and Gao, S. (2008a). World water tower: an atmospheric perspective. *Geophys. Res. Lett.* 35, 525–530. doi:10.1029/2008GL035867
- Xu, X. D., Miao, Q. J., Wang, J. Z., and Zhang, X. J. (2003). The water vapor transport model at the regional boundary during the Meiyu period. *Adv. Atmos. Sci.* 20 (3), 333–342. doi:10.1007/BF02690791
- Xu, X. D., Shi, X. Y., Wang, Y. Q., Peng, S. Q., and Shi, X. H. (2008b). Data analysis and numerical simulation of moisture source and transport associated with summer precipitation in the Yangtze River Valley over China. *Meteorol. Atmos. Phys.* 100, 217–231. doi:10.1007/s00703-008-0305-8
- Xu, X. D., Tao, S. Y., Wang, J. Z., Chen, L. S., Zhou, L., and Wang, X. R. (2002). The relationship between water vapor transport features of Tibetan Plateau-Monsoon “large triangle” affecting region and drought-flood abnormality of China (in Chinese). *Acta Meteorol. Sin.* 60(3), 257–267. doi:10.11676/qxxb2002.032
- Xu, X. D., Zhao, T. L., Lu, C. G., and Shi, X. H. (2014). Characteristics of the water cycle in the atmosphere over the Tibetan Plateau (in Chinese). *Acta Meteorol. Sin.* 72 (6), 1079–1095. doi:10.11676/qxxb2014.091
- Ye, D. Z., and Wu, G. X. (1998). The role of the heat source of the Tibetan Plateau in the general circulation. *Met Atmos Phys.* 67, 181–198. doi:10.1007/BF01277509
- Zhang, C., Tang, Q. H., and Chen, D. L. (2017). Recent changes in the moisture source of precipitation over the Tibetan Plateau. *J. Clim.* 30, 1807–1819. doi:10.1175/JCLI-D-15-0842.1
- Zhang, W. J., Jin, F. F., Li, J. P., and Ren, H. L. (2011). Contrasting impacts of two-type El Niño over the western north Pacific during boreal autumn. *J. Meteorol. Soc. Jpn.* 89, 563–569. doi:10.2151/jmsj2011-510
- Zhang, W. J., Wang, L., Xiang, B. Q., Qi, L., and He, J. H. (2015). Impacts of two types of La Niña on the NAO during boreal winter. *Clim. Dynam.* 44, 1351–1366. doi:10.1007/s00382-014-2155-z
- Zhang, Y. W., Wang, D. H., Zhai, P. M., Gu, G. J., and He, J. H. (2013). Spatial distributions and seasonal variations of tropospheric water vapor content over the Tibetan plateau. *J. Clim.* 26, 5637–5654. doi:10.1175/JCLI-D-12-00574.1
- Zhao, P., and Chen, L. X. (2001a). Climatic features of atmospheric heat source/sink over the Qinghai–Xizang Plateau in 35 years and its relation to rainfall in China. *Sci. China E.* 44 (9), 858–864. doi:10.1007/BF02907098
- Zhao, P., and Chen, L. X. (2001b). Interannual variability of atmospheric heat source/sink over the Qinghai–Xizang (Tibetan) Plateau and its relation to circulation. *Adv. Atmos. Sci.* 18(1), 106–116. doi:10.1007/s00376-001-0007-3
- Zhao, P., Xu, X. D., Chen, F., Guo, X. L., Zheng, X. D., Liu, L., et al. (2018). The third atmospheric scientific experiment for understanding the earth-atmosphere coupled system over the Tibetan Plateau and its effects. *Bull. Am. Meteorol. Soc.* 99, 757–776. doi:10.1175/BAMS-D-16-0050.1
- Zheng, X. T., Xie, S. P., and Liu, Q. Y. (2011). Response of the Indian Ocean basin mode and its capacitor effect to global warming. *J. Clim.* 24, 6146–6164. doi:10.1175/2011JCLI4169.1
- Zhou, C. Y., Deng, M. Y., and Qi, D. M. (2017). Characteristics of the moist pool over the Qinghai-Tibetan Plateau and its variation (in Chinese). *Plateau Meteorol.* 36(2), 294–306. doi:10.7522/j.issn.1000-0534.2016.00042
- Zhou, C. Y., Qi, D. M., Li, Y. Q., and Chen, D. (2015). Long-distance-relayed water vapor transport east of Tibetan plateau and its impacts. *J. Trop. Meteorol.* 21(1), 43–54. doi:10.16555/j.1006-8775.2015.01.005
- Zhou, C. Y., Zhao, P., and Chen, J. M. (2019). The interdecadal change of summer water vapor over the Tibetan Plateau and associated mechanisms. *J. Clim.* 32, 4103–4119. doi:10.1175/JCLI-D-18-0364.1
- Zhou, S. W., Wu, P., Wang, C. H., and Han, J. C. (2012). Spatial distribution of atmospheric water vapor and its relationship with precipitation in summer over the Tibetan Plateau. *J. Geogr. Sci.* 22(5), 795–809. doi:10.1007/S11442-012-0964-8
- Zhu, Z. W., Li, T., and He, J. H. (2014). Out-of-phase relationship between boreal spring and summer decadal rainfall changes in southern China. *J. Clim.* 27, 1083–1099. doi:10.1175/JCLI-D-13-00180.1

Conflict of Interest: The authors declare that the research was conducted in the absence of any commercial or financial relationships that could be construed as a potential conflict of interest.

Copyright © 2020 Ren, Zhong, Chen, Li, and Zhang. This is an open-access article distributed under the terms of the Creative Commons Attribution License (CC BY). The use, distribution or reproduction in other forums is permitted, provided the original author(s) and the copyright owner(s) are credited and that the original publication in this journal is cited, in accordance with accepted academic practice. No use, distribution or reproduction is permitted which does not comply with these terms.